Eur. Phys. J. Plus (2016) **131**: 207
DOI 10.1140/epjp/i2016-16207-3

THE EUROPEAN PHYSICAL JOURNAL PLUS

Regular Article

A modified Rusanov scheme for shallow water equations with topography and two phase flows

Kamel Mohamed[1,2,a] and F. Benkhaldoun[3,b]

[1] Mathematics Department, Faculty of Science, Taibah University, Madinah 41477, P.O. Box 30002, Saudi Arabia
[2] Permanent Address: Department of Mathematics, Faculty of Science, Assiut University, New Valley, Egypt
[3] LAGA, Université Paris 13, 99 Av.J.B.Clement, 93430 Villetaneuse, France

Received: 20 February 2016 / Revised: 29 April 2016
Published online: 22 June 2016 –

Abstract. In this work, we introduce a finite volume method for numerical simulation of shallow water equations with source terms in one and two space dimensions, and one-pressure model of two-phase flows in one space dimension. The proposed method is composed of two steps. The first, called predictor step, depends on a local parameter allowing to control the numerical diffusion. A strategy based on limiters theory enables to control this parameter. The second step recovers the conservation equation. The scheme can thus be turned to order 1 in the regions where the flow has a strong variation, and order 2 in the regions where the flow is regular. The numerical scheme is applied to several test cases in one and two space dimensions. This scheme demonstrates its well-balanced property, and that it is an efficient and accurate approach for solving shallow water equations with and without source terms, and water faucet problem.

1 Introduction

In the current work, we propose a finite volume method for solving shallow water equations, which can be used to model waves in the rivers tides, lakes, atmosphere, reservoir and open channel flows. The introduction of source terms into shallow water equations leads to numerical difficulties. To treate this problem, some authors have proposed new schemes or extensions of efficient schemes, which give good results. Several methods have been proposed, we expose some of them here. The authors of [1] modified the Roe's scheme [2] to solve the shallow water equations with source terms. This method has been improved in [3] for one-dimensional channel flows. In [4], the authors proposed the surface gradient method, which depends on the Godunov-type scheme for solving the shallow water equations with source terms. The authors of [5] proposed a quasi steady wave propagation method, which depends on the Riemann solver, in which the source terms balance with the flux gradient. A well-balanced finite volume scheme for shallow water equations with drying areas over arbitrary topography is introduced in [6]. The authors of [7], used a numerical scheme based on Godunov approach of finite volume schemes to solve the shallow water equations. In [8], the authors developed a well-balanced stable generalized Riemann problem scheme for numerical simulations of shallow water equations with irregular source terms, which aims to balance between flux gradients and bed slope topography. In [9], the authors proposed a modified predictor-corrector scheme for numerical solution of one-dimensional shallow water equations with topography. This scheme combines the weighted average flux method and the depth gradient method. A finite volume method depending on the wave-propagation algorithm is used to solve two-dimensional shallow water equations, in [10]. In [11], the authors propose a finite volume method for solutions of one and two space dimensions shallow water equations with source terms. They used an operator-splitting method to divide the governing equations into hyperbolic system and source terms. The Roe's scheme and HLL scheme are used to solve the hyperbolic equations and implicit backword Euler scheme to treat the source term. Here, we consider the one-pressure model of two phase-flows, which is represented by a non homogeneous four partial differential equations system describing mass and energy conservation. It is well known that this kind of systems has characteristics roots that can become complex. This implies that the corresponding initial value problem is not well posed. The ill-posed condition of the single-pressure models still remains a problem and challenge for practical application, many of the researchers focused on adding the

[a] e-mail: kmohamed@taibahu.edu.sa (corresponding author)
[b] e-mail: fayssal@math.univ-paris13.fr

interfacial pressure to become a hyperbolic system [12–15]. Many articles on two-phase flow models may be found in the literature. For example, in [16], the authors presented the computational framework for solving hyperbolic models for compressible two-phase flow by finite volume methods (MUSCL-Hancock methods). In [17], the authors used a well-balanced scheme (Lax-Friefrichs) for solving two-phase flows models, where one phase is compressible and the other is incompressible. The system is a closed system with four governing equations for four unknowns. In this paper, we develop a finite volume method to solve the shallow water equations with and without source terms in one and two space dimensions, and one-pressure model of two-phase flows. This method uses an extension of the two steps flux scheme [18], which depends on a local adjustable parameter $\alpha^n_{j+\frac{1}{2}}$. The origin of this scheme has been recently proposed by [19,20]. The stability analysis of the scheme show that the scheme can be of order one or order two according to the value of the parameter of control $\alpha^n_{j+\frac{1}{2}}$ [21]. A strategy of variation of this parameter is based on the limiters theory. There are many advantages of the proposed scheme. First, this scheme is capable to satisfy the exact C-property. Second, this method uses only physical flux computation and average states instead of Jacobian eigenvectors. Third, this method is simple to implement and accurate. Finally, it avoids the solution of Riemann problems during the time integration process. This paper is organized as follows: In sect. 2, the shallow water equations with source terms in one dimension are considered, this section also includes the construction of finite volume numerical scheme for shallow water equations with source terms and treatment of the source term. In sect. 3, we introduce the two-dimensional system of shallow water equations with source terms and the construction of the finite volume scheme in two dimension together. The applications of modified Rusanov scheme in one and two dimensions is included in sects. 4 and 5. In sect. 6, we introduce a two-phase flow model in one dimension and a modified Rusanov scheme algorithm for this model. Section 7 summarizes our work and gives concluding remarks.

2 One-dimensional shallow water equations with topography

The shallow water equations with topography in one dimension can be written in conservation form as follows:

$$\frac{\partial \mathbf{W}}{\partial t} + \frac{\partial \mathbf{F}(\mathbf{W})}{\partial x} = \mathbf{Q}(\mathbf{W}), \tag{1}$$

where $\mathbf{W}$ is the conserved variable, $\mathbf{F}(\mathbf{W})$ is the physical flux and $\mathbf{Q}(\mathbf{W})$ is the source term. They are given by

$$\mathbf{W} = \begin{pmatrix} h \\ hu \end{pmatrix}, \qquad \mathbf{F}(\mathbf{W}) = \begin{pmatrix} hu \\ hu^2 + \frac{1}{2}gh^2 \end{pmatrix}, \qquad \mathbf{Q}(\mathbf{W}) = \begin{pmatrix} 0 \\ Q_0 + Q_f \end{pmatrix}, \tag{2}$$

where h is the water height, u is the water velocity, g is the acceleration due to gravity. Q_0 and S_f are the source terms corresponding to the bottom slope and the friction, respectively, defined as

$$Q_0 = -gh\frac{\partial Z}{\partial x}, \qquad Q_f = gh\eta^2\frac{u^2}{h^{\frac{4}{3}}},$$

where Z is the bottom elevation and η is the Manning roughness coefficient. Here, we neglect Q_f. The eigenvalues of the Jacobian matrix

$$A(W) = \frac{\partial \mathbf{F}(\mathbf{W})}{\partial \mathbf{W}} = \begin{pmatrix} 0 & 1 \\ c^2 - u^2 & 2u \end{pmatrix},$$

are

$$\lambda_1 = u - c, \qquad \lambda_2 = u + c, \tag{3}$$

where $c = \sqrt{gh}$ is the gravity wave speed. This eigenvalues correspond to the propagation velocities of the various components of the wave and are often called characteristic speed.

2.1 Well-balanced modified Rusanov method

To formulate the finite volume method, we discretize the spatial domain into control volume $\Delta x = x_{i+1/2} - x_{i-1/2}$ and we divide the time interval into sub intervals $[t_n, t_{n+1}]$ with uniform size Δt. We integrate the considered eq. (1) with respect to time and space over the domain $[t_n, t_{n+1}] \times [x_{i-1/2}, x_{i+1/2}]$ to obtain the following discrete equation:

$$W_i^{n+1} = W_i^n - \frac{\Delta t}{\Delta x}\left(F\left(W^n_{i+1/2}\right) - F\left(W^n_{i-1/2}\right)\right) + \Delta t {Q_i}^n, \tag{4}$$

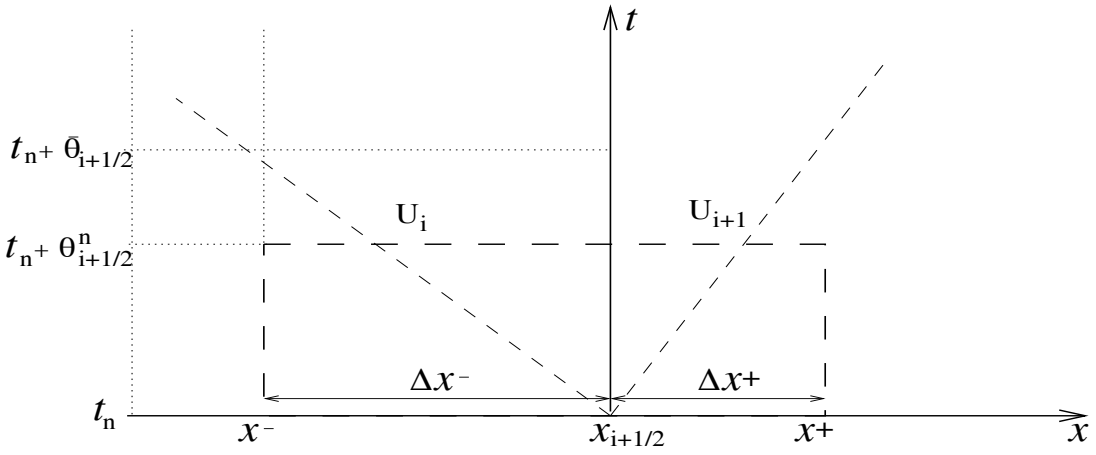

Fig. 1. The control space-time domain in the modified Rusanov method.

where W_i^n is the average of the solution W in the domain $[x_{i-1/2}, x_{i+1/2}]$ at time t_n, *i.e.*

$$W_i^n = \frac{1}{\Delta x}\int_{x_{i-1/2}}^{x_{i+1/2}} W(t_n, x)\,\mathrm{d}x,$$

and $F(W^n_{i\pm1/2})$ is the numerical flux at $x = x_{i\pm1/2}$ and time t_n. The spatial discretization of eq. (4) is completed when a numerical construction of the fluxes $F(W^n_{i\pm1/2})$ is chosen and a discretization of the source term ${Q_i}^n$ is performed. In general, the construction of the numerical fluxes $F(W^n_{i\pm1/2})$ in the finite volume discretization (4) requires a solution of Riemann problems at the cell interfaces $x_{i\pm1/2}$. Let us assume that the self-similar solution to the Riemann problem associated with eq. (1) subject to the initial condition

$$W(x,0) = \begin{cases} W_L, & \text{if} \quad x < 0, \\ W_R, & \text{if} \quad x > 0, \end{cases} \tag{5}$$

is given by

$$W(t,x) = R_s\left(\frac{x}{t}, W_L, W_R\right),$$

where R_s is the Riemann solution which has to be either calculated exactly or approximated. Thus, the intermediate state $W^n_{i+1/2}$ in (4) at the cell interface $x = x_{i+1/2}$ is defined as

$$W^n_{i+1/2} = R_s\left(0, W_i^n, W_{i+1}^n\right). \tag{6}$$

From a computational viewpoint, this procedure is very demanding and may restricts the application of the method for which Riemann solutions are difficult to approximate or simply are not available. In order to avoid these numerical difficulties and reconstruct an approximation of $W^n_{i+1/2}$, we adapt a modified Rusanov method proposed in [21–24] for numerical solution of conservation laws with source terms. The central idea is to integrate eq. (1) over a control domain $[t_n, t_n + \theta^n_{i+1/2}] \times [x^-, x^+]$ containing the point $(t_n, x_{i+1/2})$ as depicted in fig. 1. Notice that the integration of eq. (1) over the control domain $[t_n, t_n+\theta^n_{i+1/2}]\times[x^-, x^+]$ is used only at a predictor stage to construct the intermediate states $W^n_{i\pm1/2}$ which will be used in the corrector stage (4). Here, $W^n_{i\pm1/2}$ can be viewed as an approximation of the averaged Riemann solution R_s over the control volume $[x^-, x^+]$ at time $t_n + \theta^n_{i+1/2}$. Thus, the resulting intermediate state is given by

$$\begin{aligned}\int_{x^-}^{x^+} W(t_n + \theta^n_{i+1/2}, x)\,\mathrm{d}x = {} & \Delta x^- W_i^n + \Delta x^+ W_{i+1}^n \\ & - \theta^n_{i+1/2}\left(F(W^n_{i+1}) - F(W_i^n)\right) + \theta^n_{i+1/2}(\Delta x^- - \Delta x^+)Q^n_{i+\frac{1}{2}},\end{aligned} \tag{7}$$

where the distance measures Δx^- and Δx^+ as

$$\Delta x^- = \left|x^- - x_{i+1/2}\right|, \qquad \Delta x^+ = \left|x^+ - x_{i+1/2}\right|,$$

and $Q^n_{i+\frac{1}{2}}$ is an approximation of the averaged source term Q

$$Q^n_{i+\frac{1}{2}} = \frac{1}{\theta^n_{i+\frac{1}{2}}(\Delta x^- + \Delta x^+)} \int_{t-n}^{t_n+\theta^n_{i+\frac{1}{2}}} \int_{x^-}^{x^+} Q(W)\mathrm{d}t\,\mathrm{d}x. \tag{8}$$

By setting $x^- = x_i$ and $x^+ = x_{i+1}$, eq. (7) reduces to

$$W^n_{i+1/2} = \frac{1}{2}\left(W^n_i + W^n_{i+1}\right) - \frac{\theta^n_{i+1/2}}{\Delta x}\left(F(W^n_{i+1}) - F(W^n_i)\right) + \theta^n_{i+\frac{1}{2}} Q^n_{i+\frac{1}{2}}, \tag{9}$$

where $W^n_{i+1/2}$ is an approximate average of the solution W in the control domain $[t_n, t_n + \theta^n_{i+1/2}] \times [x_i, x_{i+1}]$ defined as

$$W^n_{i+1/2} = \frac{1}{\Delta x}\int_{x_i}^{x_{i+1}} W(x, t_n + \theta^n_{i+1/2})\mathrm{d}x. \tag{10}$$

Note that other selections for x^- and x^+ in (7) are also possible. In order to complete the implementation of the above finite volume method, the time parameter $\theta^n_{i+1/2}$ has to be selected. Based on the stability analysis reported in [21] for conservation laws, the variable $\theta^n_{j+1/2}$ is selected as

$$\theta^n_{i+1/2} = \alpha^n_{i+1/2}\bar{\theta}_{i+1/2}, \qquad \bar{\theta}_{i+1/2} = \frac{\Delta x}{2S^n_{i+1/2}}, \tag{11}$$

where $\alpha^n_{i+1/2}$ is a positive parameter to be calculated locally and $S^n_{i+1/2}$ is the local Rusanov velocity defined as

$$S^n_{i+1/2} = \max_{k=1,\ldots,K}\left(\max(|\lambda^n_{k,i}|, |\lambda^n_{k,i+1}|)\right), \tag{12}$$

with $\lambda^n_{k,i}$ is the k-th eigenvalue in (3). Notice that the introduction of the local time step $\theta^n_{i+1/2}$ in the predictor stage (9) is motivated by the fact that $\theta^n_{i+1/2}$ should not be larger than the value of $\bar{\theta}_{i+1/2}$ which corresponds to the time required for the fastest wave generated at the interface $x_{i+1/2}$ to leave the cell $[x_i, x_{i+1}]$, see fig. 1. It is clear that by setting $\alpha^n_{i+1/2} = 1$, the proposed finite volume method reduces to a first-order scheme, whereas for $\alpha^n_{i+1/2} = \frac{\Delta t}{\Delta x}S^n_{i+1/2}$ one recovers the well-known Lax-Wendroff scheme [25]. Another choice of the slopes $\alpha^n_{i+1/2}$ leading to a first-order scheme is $\alpha^n_{i+1/2} = \tilde{\alpha}^n_{i+1/2}$, with

$$\tilde{\alpha}^n_{i+1/2} = \frac{S^n_{i+1/2}}{s^n_{i+1/2}}, \tag{13}$$

where

$$s^n_{i+1/2} = \min_{k=1,\ldots,K}\left(\max(|\lambda^n_{k,i}|, |\lambda^n_{k,i+1}|)\right). \tag{14}$$

In the present work, we consider a second-order scheme incorporating limiters in its reconstruction as

$$\alpha^n_{i+1/2} = \tilde{\alpha}^n_{i+1/2} + \sigma^n_{i+1/2}\Phi\left(r^m_{i+1/2}\right), \tag{15}$$

where $\tilde{\alpha}^n_{i+1/2}$ is given by (13) and $\Phi_{i+1/2} = \Phi(r^m_{i+1/2})$ is an appropriate limiter which is defined by using a flux limiter function Φ acting on a quantity that measures the ratio $r^m_{i+1/2}$ of the upwind change to the local change, see for instance [26]. Thus,

$$\sigma^n_{i+1/2} = \frac{\Delta t}{\Delta x}S^n_{i+1/2} - \frac{S^n_{i+1/2}}{s^n_{i+1/2}},$$

then, the parameter of control can be written as

$$\alpha^n_{i+1/2} = \left(1 - \Phi\left(r^m_{i+1/2}\right)\right)\frac{S^n_{i+1/2}}{s^n_{i+1/2}} + \frac{\Delta t}{\Delta x}S^n_{i+1/2}\Phi\left(r^m_{i+1/2}\right), \tag{16}$$

and the ratio of the upwind change dependent on Riemann invariants and is calculated locally as

$$r^m_{i+1/2} = \frac{U^m_{i+1-q} - U^m_{i-q}}{U^m_{i+1} - U^m_i}, \quad q = \mathrm{sgn}\left[F'(U^n_{i+1/2})\right],$$

where $U^m = u + (-1)^m 2\sqrt{gh}$ is the Riemann Invariants and $m = 1, 2$. As slope limiter functions, we consider the Minmod function

$$\Phi(r) = \max\left(0, \min(1, r)\right), \tag{17}$$

the Superbee function

$$\Phi(r) = \max\left(0, \min(1, 2r), \min(2, r)\right), \tag{18}$$

Van Leer

$$\Phi(r) = \frac{r + |r|}{1 + r}, \tag{19}$$

and the van Albada function

$$\Phi(r) = \frac{r + r^2}{1 + r^2}. \tag{20}$$

The reconstructed slopes (15) are inserted in (11) and the numerical fluxes $W^n_{i+1/2}$ are computed from (9). Remark that if we set $\Phi = 0$, the spatial discretization (15) reduces to the first-order scheme.

Finally, we write our scheme for shallow water equations with topography as

$$\begin{cases} W^n_{i+\frac{1}{2}} = \dfrac{1}{2}\left(W^n_i + W^n_{i+1}\right) - \dfrac{\alpha^n_{i+\frac{1}{2}}}{2S^n_{i+\frac{1}{2}}}\left[F(W^n_{i+1}) - F(W^n_i)\right] - \dfrac{\alpha^n_{i+\frac{1}{2}}}{4S^n_{i+\frac{1}{2}}}\left(h^n_i + h^n_{i+1}\right)\left(Z_{i+1} - Z_i\right) \\ W^{n+1}_i = W^n_i - r^n\left[F\left(W^n_{i+\frac{1}{2}}\right) - F\left(W^n_{i-\frac{1}{2}}\right)\right] - g\dfrac{\Delta t^n}{8\Delta x}\left(h^n_{i+1} + 2h^n_i + h^n_{i-1}\right)\left(Z_{i+1} - Z_{i-1}\right). \end{cases} \tag{21}$$

2.2 Approximation of the source term

The numerical scheme satisfies C-property for eq. (1), if the conditions

$$u^n = 0 \quad \text{and} \quad h^n + Z = \text{const.} \tag{22}$$

hold for stationary flows at rest, see [1] and [27].

In the proposed finite volume scheme, the approximation of the source term in the corrector stage is reconstructed such that, the C-property is satisfied, to obtain stationary flows at rest, we put, $u = 0$, then the system (1) becomes

$$\frac{\partial}{\partial t}\begin{pmatrix} h \\ 0 \end{pmatrix} + \frac{\partial}{\partial x}\begin{pmatrix} 0 \\ \frac{1}{2}gh^2 \end{pmatrix} = \begin{pmatrix} 0 \\ -gh\dfrac{\partial}{\partial x}Z \end{pmatrix} = Q(x, t). \tag{23}$$

Applying the modified Rusanov scheme to eq. (23), we can write the predictor stage (9) as

$$W^n_{i+\frac{1}{2}} = \begin{pmatrix} \dfrac{1}{2}(h^n_i + h^n_{i+1}) \\ -\dfrac{\alpha^n_{i+\frac{1}{2}}}{4S^n_{i+\frac{1}{2}}} g(h^n_{i+1} + h^n_i)[h^n_{i+1} - h^n_i + Z_{i+1} - Z_i] \end{pmatrix} = \begin{pmatrix} \dfrac{1}{2}(h^n_i + h^n_{i+1}) = h^n_{i+\frac{1}{2}} \\ 0 \end{pmatrix}, \tag{24}$$

and the corrector stage updates the solution written as

$$\begin{pmatrix} h^{n+1}_i \\ q^{n+1}_i \end{pmatrix} = \begin{pmatrix} h^n_i \\ q^n_i \end{pmatrix} - \frac{rg}{2}\begin{pmatrix} 0 \\ \left(h^n_{i+\frac{1}{2}}\right)^2 - \left(h^n_{i-\frac{1}{2}}\right)^2 \end{pmatrix} + \begin{pmatrix} 0 \\ \Delta t_n Q^n_i \end{pmatrix}, \tag{25}$$

the solution remains stationary when $W^{n+1}_i = W^n_i$, the discretisation of the source term and the flux must cancel out, then the previous equation can be written as follows:

$$\frac{r}{2}g\left(\left(h^n_{i+\frac{1}{2}}\right)^2 - \left(h^n_{i-\frac{1}{2}}\right)^2\right) - \Delta t_n Q^n_i,$$

and then

$$Q^n_i = -\frac{g}{8\Delta x}\left(h^n_{i+1} + 2h^n_i + h^n_{n-1}\right)\left(Z_{i+1} - Z_{i-1}\right).$$

Hence, if the source term in the corrector stage is discretized in the previous form, then the proposed scheme satisfies the C-property.

3 Two-dimensional shallow water equations with topography

The two-dimensional shallow water equations with source term can be written as

$$\frac{\partial \mathbf{W}}{\partial t} + \frac{\partial \mathbf{F}(\mathbf{W})}{\partial x} + \frac{\partial \mathbf{G}(\mathbf{W})}{\partial y} = \mathbf{Q}(\mathbf{W}), \tag{26}$$

where $\mathbf{W}$ is the conserved variable, $\mathbf{F}(\mathbf{W})$ and $\mathbf{G}(\mathbf{W})$ are the physical fluxes and $\mathbf{Q}(\mathbf{W})$ is the source term, which are given by

$$\mathbf{W} = \begin{pmatrix} h \\ hu \\ hv \end{pmatrix}, \qquad \mathbf{F}(\mathbf{W}) = \begin{pmatrix} hu \\ hu^2 + \frac{1}{2}gh^2 \\ huv \end{pmatrix},$$

$$\mathbf{G}(\mathbf{W}) = \begin{pmatrix} hv \\ huv \\ hv^2 + \frac{1}{2}gh^2 \end{pmatrix}, \qquad \mathbf{Q}(\mathbf{W}) = \begin{pmatrix} 0 \\ Q_{0,x} + Q_{f,x} \\ Q_{0,y} + Q_{f,y} \\ 0 \end{pmatrix},$$

where h is the water height, u and v are the velocities in the x and y directions, $Q_{0,x}$ and $Q_{0,y}$ are the bed slope variation in the x and y directions, $Q_{f,x}$ and $Q_{f,y}$ are the source terms arising from friction. They are given by

$$\begin{aligned} Q_{0,x} &= -gh\frac{\partial Z}{\partial x}, \\ Q_{0,y} &= -gh\frac{\partial Z}{\partial y}, \\ Q_{f,x} &= gh\eta^2\frac{u\sqrt{u^2+v^2}}{h^{\frac{4}{3}}}, \\ Q_{f,y} &= gh\eta^2\frac{v\sqrt{u^2+v^2}}{h^{\frac{4}{3}}}, \end{aligned}$$

where η is the Manning roughness coefficient. Here, we neglect $Q_{f,x}$ and $Q_{f,y}$. The Jacobian matrix of the system of eqs. (26) can be written as follows:

$$\begin{aligned} & A(W,\vec{n}) = A_1(W)n_x + A_2(W)n_y = \frac{\partial \mathbf{F}(\mathbf{W})}{\partial \mathbf{W}}n_x + \frac{\partial \mathbf{G}(\mathbf{W})}{\partial \mathbf{W}}n_y \\ \therefore \quad & A(W,\vec{n}) = \begin{pmatrix} 0 & n_x & n_y \\ (c^2-u^2)n_x - uvn_y & 2un_x + vn_y & un_y \\ -uvn_x + (c^2-v^2)n_y & vn_x & un_x + 2vn_y \end{pmatrix}. \end{aligned}$$

The eigenvalues of this matrix are given by

$$\lambda_1 = un_x + vn_y - c, \quad \lambda_2 = un_x + vn_y, \quad \text{and} \quad \lambda_3 = un_x + vn_y + c,$$

where $c = \sqrt{gh}$.

3.1 Well-balanced modified Rusanov method in two dimensions

We integrate eq. (26) on a generic control volume C_i, that result from the discretization of the computational domain into a number of control volume,

$$\int_{C_i}\left(\frac{\partial W}{\partial t} + \frac{\partial F(W)}{\partial x} + \frac{\partial G(W)}{\partial x}\right)\mathrm{d}x\,\mathrm{d}y = \int_{C_i} Q(x,y,W)\,\mathrm{d}x\,\mathrm{d}y.$$

From the divergence theorem, we obtain

$$\int_{C_i}\frac{\partial W}{\partial t}\,\mathrm{d}x\,\mathrm{d}y + \int_{\delta C_i}(F(W)n_x + G(W)n_y)\,\mathrm{d}\sigma = \int_{C_i} Q(x,y,W)\,\mathrm{d}x\,\mathrm{d}y.$$

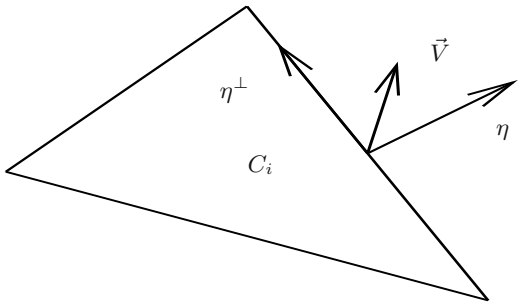

Fig. 2. A generic control volume C_i.

Let $\mathcal{F}(W,\vec{n}\,) = F(W)n_x + G(W)n_y$ and we suppose that W_i is constant per cell (mean value of W in the cell C_i). So, we get

$$A_i\frac{\partial W_i}{\partial t} + \sum_{j\in K(i)}\int_{\gamma_{ij}} \mathcal{F}(W,\vec{n}\,)\mathrm{d}\sigma = \int_{C_i} Q(x,y,W)\mathrm{d}x\,\mathrm{d}y,$$

where A_i is the area of the cell C_i and $K(i)$ is the set of neighboring triangles of the cell C_i, with $\vec{n} = (n_x, n_y)^t$ is the unit outward normal to the surface δC_i. Following similar formalism as in one-dimension, we can define the numerical flux as

$$\int_{\gamma_{ij}} \mathcal{F}(W,\vec{n}\,)\,\mathrm{d}\sigma = \phi(W_i^n, W_j^n, \overrightarrow{n_{ij}})\,\mathrm{mes}(\gamma_{ij}),$$

where $\mathrm{mes}(\gamma_{ij})$ is the length of the edge γ_{ij}. Finally, we can write the corrector stage of the scheme as

$$W_i^{n+1} = W_i^n - \frac{\Delta t_n}{A_i}\sum_{j\in K(i)} \phi(W_i^n, W_j^n, \vec{n_{ij}})\,\mathrm{mes}(\gamma_{ij}) + \Delta t_n Q_i^n, \tag{27}$$

with $Q_i^n = \frac{1}{A_i}\int_{C_i} Q(x,y,W)\,\mathrm{d}x\,\mathrm{d}y$ and $\phi(W_i^n, W_j^n, \vec{n_{ij}})$ is the two-dimensional numerical flux.

Our goal here is to write the numerical flux in a similar way to the one-dimensional case. We can write $\phi(W_i^n, W_j^n, \vec{n}_{ij}) = \mathcal{F}(W_{ij}^n, \vec{n}_{ij})$, where W_{ij}^n is determined at the predictor stage. To determine the W_{ij}^n, we project eq. (26) on the local outward normal η and tangential $\eta^{\perp}$ as in fig. 2.

We get

$$\begin{cases} \dfrac{\partial h}{\partial t} + \dfrac{\partial hU}{\partial \eta} = 0, \\ \dfrac{\partial hU}{\partial t} + \dfrac{\partial (hU^2 + \frac{1}{2}gh^2)}{\partial \eta} + gh\dfrac{\mathrm{d}Z}{\mathrm{d}\eta} = 0, \\ \dfrac{\partial hV}{\partial t} + \dfrac{\partial hUV}{\partial \eta} = 0, \end{cases} \tag{28}$$

where $U = \vec{V}\cdot\eta = un_x + vn_y$ and $V = \vec{V}\cdot\eta^{\perp} = -un_y + vn_x$ are the normal and tangential velocity, respectively. We can write the predictor stage using $M_{ij}(X) = \frac{1}{2}(X_i + X_j)$ and $\Delta_{ij}(X) = X_j - X_i$ as follows:

$$\begin{cases} (h)_{ij} = M_{ij}(h) - \dfrac{\alpha_{ij}^n}{2S_{ij}^n}\Delta_{ij}(hU), \\ (hU)_{ij} = M_{ij}(hU) - \dfrac{\alpha_{ij}^n}{2S_{ij}^n}\Delta_{ij}\left(hU^2 + \dfrac{1}{2}gh^2\right) - \dfrac{\alpha_{ij}^n}{2S_{ij}^n}g(\tilde{h})_{ij}\Delta_{ij}(Z), \\ (hV)_{ij} = M_{ij}(hV) - \dfrac{\alpha_{ij}^n}{2S_{ij}^n}\Delta_{ij}(hUV), \end{cases} \tag{29}$$

where $\tilde{h}_{ij} = \frac{A_i h_i + A_j h_j}{A_i + A_j}$ is the linear approximation of h_i and h_j with A_i is the area of cell C_i. The solution W_{ij}^n is recovered by using the following transformation:

$$(hu)_{ij} = n_x(hU)_{ij} - n_y(hV)_{ij}$$

and

$$(hv)_{ij} = n_y(hU)_{ij} + n_x(hV)_{ij}.$$

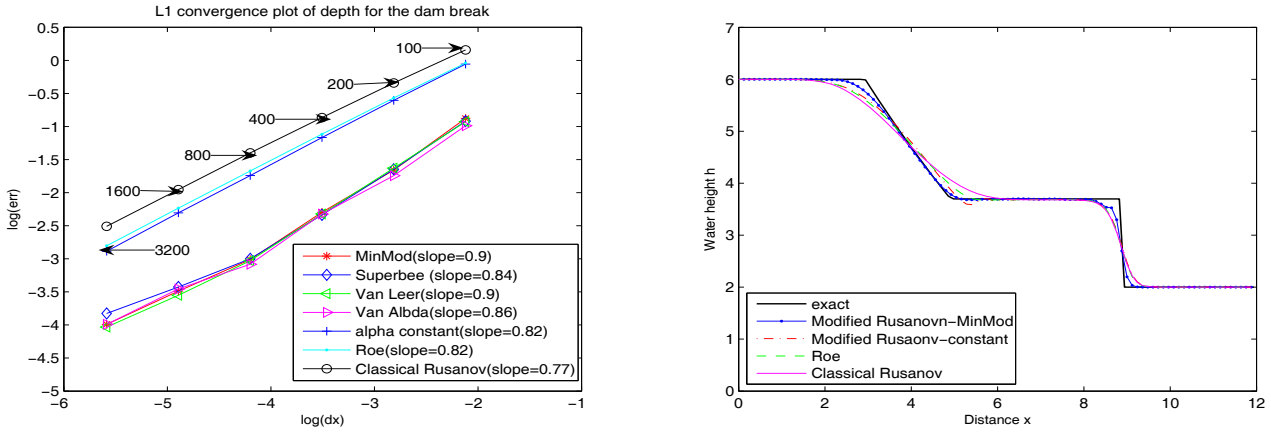

Fig. 3. (a) L_1 convergence of the water height in dam break. (b) Comparative results for water height in dam break at $t = 0.4$ s.

4 Numerical results in one dimension

We introduce numerical results for a test problem to check the performance and the accuracy of the proposed finite volume method. As with all explicit time stepping methods the theoretical maximum stable time step Δt is specified according to the CFL condition

$$\Delta t = Cr \frac{\Delta x}{\max_i \left(\left| \alpha^n_{i+1/2} S^n_{i+1/2} \right| \right)}, \tag{30}$$

where Cr is a constant, called Courant number to be chosen less than unity, and the time step is varied according to eq. (30).

4.1 Test 1

This test case consists of a one-dimensional channel of length 12 m and the initial conditions are given as

$$u(0,x) = 0 \quad \text{and} \quad h(0,x) = \begin{cases} 6, & \text{if} \quad x \leq 6 \\ 2, & \text{if} \quad x > 6. \end{cases} \tag{31}$$

The solution of this problem consists of a rarefaction wave and shock wave which are traveling upstream and downstream, respectively. We run the modified Rusanov scheme, Roe's scheme and Rusanov's scheme using six different meshes of size $\Delta x = 0.12, 0.06, 0.03, 0.015, 0.0075$ and 0.00375, respectively.

Figure 3(a) shows an error convergence plot in the L_1 norm for the water height, the curve has slope slightly in access of 0.9, 0.84, 0.9 and 0.86 for the modified Rusanov scheme with parameter of control $\alpha^n_{j+\frac{1}{2}}$, which is modulated using the Minmod, Superbee, Van Leer and Van Albda limiter, respectively, 0.82 for modified Rusanov with constant $\alpha^n_{j+\frac{1}{2}}$, 0.82 for the Roe scheme and 0.77 for the classical Rusanov scheme. We note small differences in respect to the choice of the limiter and we obtain a good accuracy with the modified Rusanov with parameter of control $\alpha^n_{j+\frac{1}{2}}$, while the error is less than the error of Roe's scheme, modified Rusanov with constant parameter and classical Rusanov scheme. Figure 3(b) shows comparison of the numerical solution with modified Rusanov scheme, Roe's scheme [2] and Rusanov's scheme [28] with exact solution at time $t = 0.4$, we note that the modified Rusanov scheme with parameter of control $\alpha^n_{j+\frac{1}{2}}$ produces numerical results thet are more accurate the those computed using the Roe scheme, the modified Rusanov scheme with constant parameter or Rusanov's scheme. Also, it produces numerical results as accurate as those computed using Roe's scheme. Figure 4(a) depicts the water velocity for numerical solution of different schemes and exact solution at time $t = 0.4$, the numerical results are in good agreement with the exact solution. Figure 4(b) shows the variation of parameter of control $\alpha^n_{j+\frac{1}{2}}$, this variation has been detected in the area on the computational domain where the rarefaction and shock waves appear.

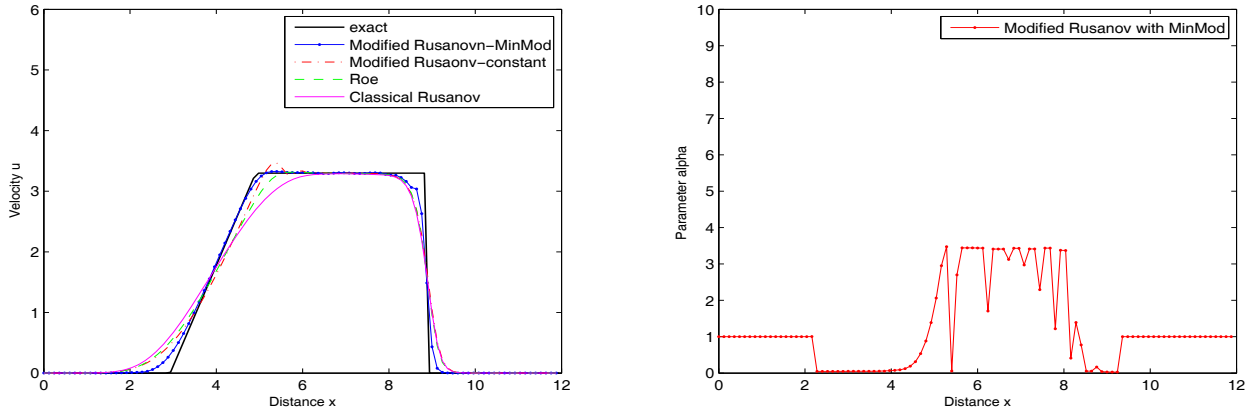

Fig. 4. (a) Water velocity (left) for dam break. (b) parameter of control $\alpha^n_{j+\frac{1}{2}}$ computed with 100 celles at $t = 0.4\,\mathrm{s}$.

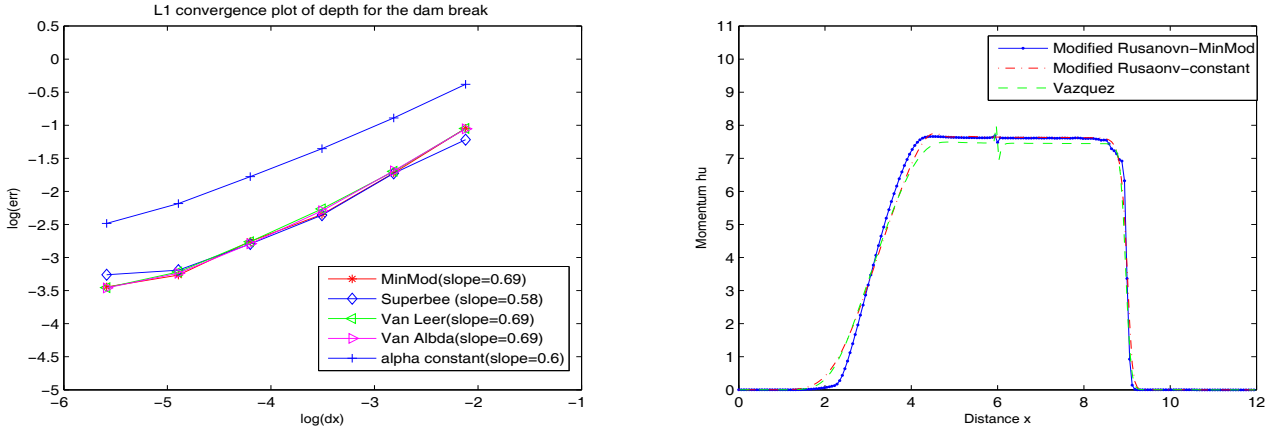

Fig. 5. (a) L_1 convergence of the water height in dam break. (b) Comparative results for discharge in dam break at $t = 0.4\,\mathrm{s}$.

4.2 Test 2

This test case consists of a one-dimensional dam break over a step and was presented in [29], it corresponds to a Riemann problem with a singular source function and the initial conditions are given by

$$h(0,x) = \begin{cases} 5, & \text{if} \quad x \leq 6 \\ 1, & \text{if} \quad x > 6, \end{cases} \qquad u(0,x) = 0 \quad \text{and} \quad Z = \begin{cases} 0, & \text{if} \quad x \leq 6 \\ 1, & \text{if} \quad x > 6. \end{cases} \tag{32}$$

The exact solution of this test is computed in [29] and for the data above the solution consists of a rarefaction, a stationary linear discontinuity at the bed step and a travelling shock wave. We run the modified Rusanov scheme and Vazquez's scheme at time $t = 0.4$. Figure 5(a) shows an error convergence plot in the L_1 norm for the water height, the curve have slope slightly in access of 0.69, 0.58, 0.69 and 0.69 for the modified Rusanov scheme with parameter of control $\alpha^n_{j+\frac{1}{2}}$ modulated using the Minmod, Superbee, Van Leer and Van Albda limiter, respectively, and 0.6 for modified Rusanov with constant $\alpha^n_{j+\frac{1}{2}}$. We note small differences with the choice of the limiter and we obtain a good accuracy with the modified Rusanov scheme with parameter of control $\alpha^n_{j+\frac{1}{2}}$ and the error is less than modified Rusanov with constant parameter. Figure 4(a) shows the comparison for discharge $q = hu$ and exact solution. Figure 5(b) depicts the water discharge $q = hu$ numerical solution with modified Rusanov, Vazquez's scheme and exact solution computed with 100 cell and time $t = 0.4$, these results are in good agreement with the exact solution but there is a high level of oscillations with the Vazquez's scheme, which is due to the irregular bottom and which can not be handled because the imbalance between the flux term and source term.

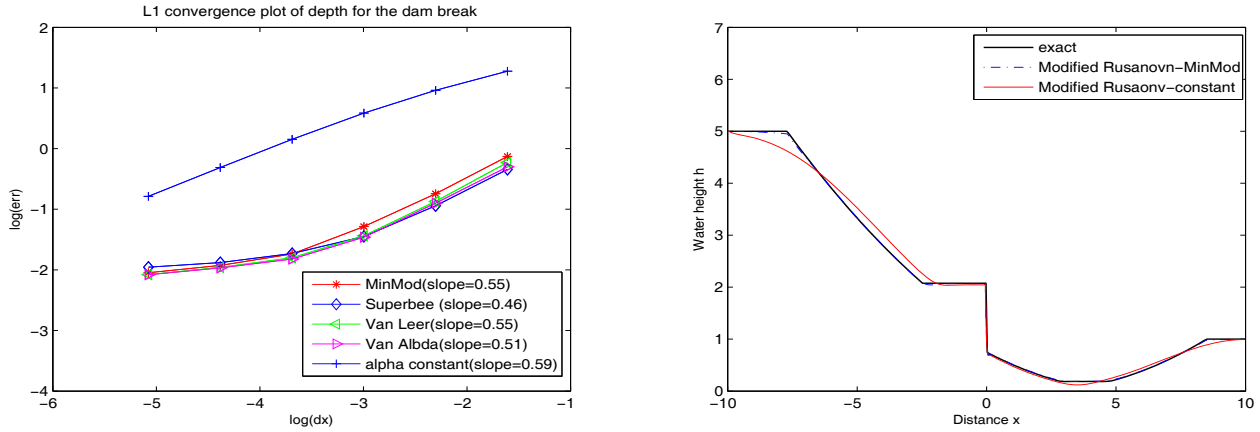

Fig. 6. (a) L_1 convergence of the water height in dam break. (b) Comparative results for water velocity in dam break at $t = 0.7\,\mathrm{s}$.

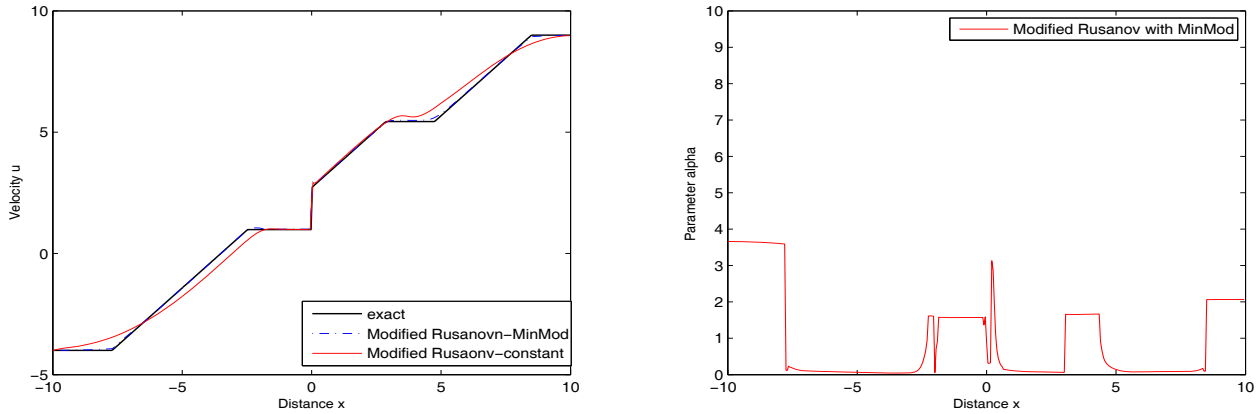

Fig. 7. (a) Water velocity for dam break. (b) Parameter of control (right) $\alpha^n_{j+\frac{1}{2}}$ computed with 100 celles at $t = 0.7\,\mathrm{s}$.

4.3 Test 3

This test is a transcritical case which consists of a one-dimensional dam break over a step and was presented in [29] with the initial conditions defined as

$$h(0,x) = \begin{cases} 5, & \text{if} \quad x \leq 6 \\ 1, & \text{if} \quad x > 6, \end{cases} \qquad u(0,x) = \begin{cases} -4, & \text{if} \quad x \leq 6 \\ 9, & \text{if} \quad x > 6, \end{cases} \tag{33}$$

$$\text{and} \quad Z(0,x) = \begin{cases} 0, & \text{if} \quad x \leq 6 \\ 1, & \text{if} \quad x > 6. \end{cases} \tag{34}$$

The exact solution of this test is computed in [29]. We have run the modified Rusanov scheme using six different meshes of size $\Delta x = 0.2, 0.1, 0.05, 0.025, 0.0125$ and 0.00625, respectively, at time $t = 0.7\,\mathrm{s}$. Figure 6(a) shows an error convergence plot in the L_1 norm for the water height, the curve has slope slightly in access of 0.55, 0.46, 55, 0.51 for the modified Rusanov scheme with the parameter of control $\alpha^n_{j+\frac{1}{2}}$ being modulated using the Minmod, Superbee, Van Leer and Van Albda limiter respectively and 0.59 for modified Rusanov with constant $\alpha^n_{j+\frac{1}{2}}$. We note small differences with respect to the choice of the limiter parameter and we obtain a good accuracy with the modified Rusanov with parameter of control $\alpha^n_{j+\frac{1}{2}}$. The obtained error is less than the one with the modified Rusanov scheme with a constant parameter. Figure 6(b) shows comparison between the numerical solution with the modified Rusanov scheme and exact solution using 400 cells and time $t = 0.7\,\mathrm{s}$, we also note that the modified Rusanov with parameter of control $\alpha^n_{j+\frac{1}{2}}$ produces numerical results more accurate those computed using the modified Rusanov scheme with a constant parameter of control. Figure 7(a) shows comparisons on water velocity between the numerical solution with modified

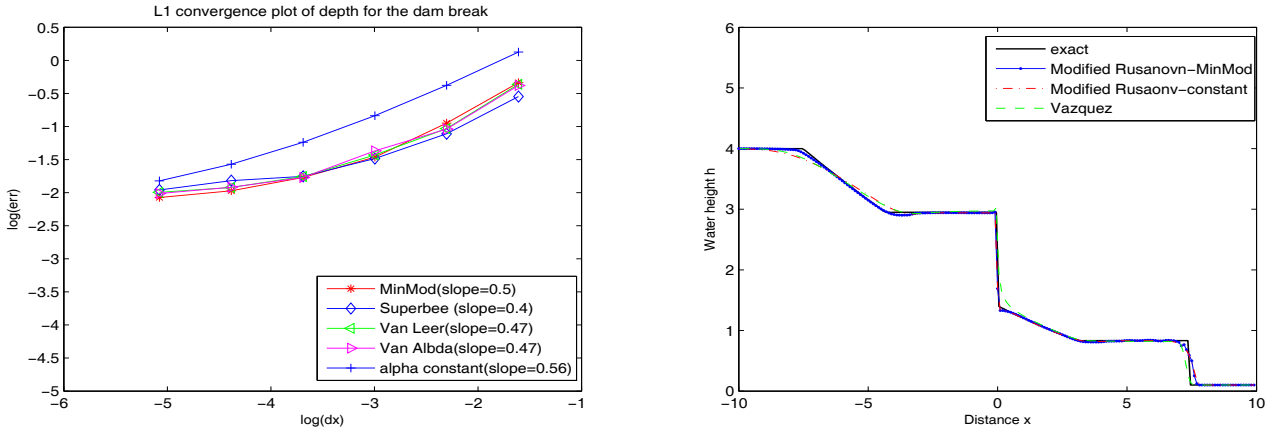

Fig. 8. (a) L_1 convergence of the water height in dam break. (b) Comparative results for water height in dam break at $t = 1.2\,\mathrm{s}$.

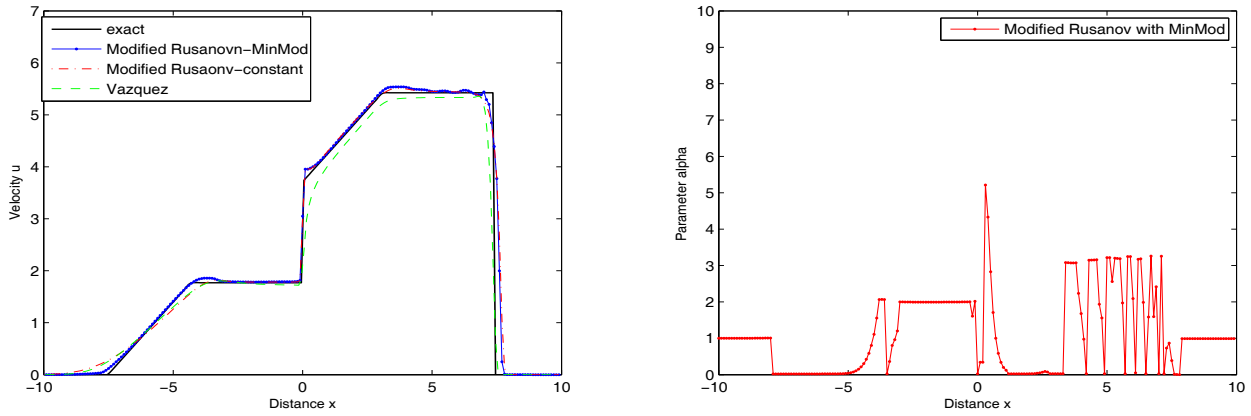

Fig. 9. (a) Water velocity for dam break. (b) Parameter of control $\alpha^n_{j+\frac{1}{2}}$ computed with 100 celles at $t = 1.2\,\mathrm{s}$.

Rusanov scheme and exact solution using 400 cells and time $t = 0.7$. We note that the modified Rusanov scheme with parameter of control $\alpha^n_{j+\frac{1}{2}}$ produces numerical results that are more accurate than those computed using the modified Rusanov scheme with constant parameter. Figure 7(b) shows the variation of the parameter of control $\alpha^n_{j+\frac{1}{2}}$. This variation has been detected in the area on the computational domain of important variation of the solution.

4.4 Test 4

This test case consists of a one-dimensional dam break over a step and was presented in [29] and the initial conditions are given by

$$h(0,x) = \begin{cases} 4, & \text{if} \quad x \leq 6 \\ 0.1, & \text{if} \quad x > 6, \end{cases} \qquad u(0,x) = 0 \quad \text{and} \quad Z = \begin{cases} 0, & \text{if} \quad x \leq 6 \\ 1, & \text{if} \quad x > 6. \end{cases} \tag{35}$$

We have run the modified Rusanov scheme and Vazquez's scheme using six different meshes of size $\Delta x = 0.2, 0.1, 0.05, 0.025, 0.0125$ and 0.00625, respectively, at time $t = 1.2\,\mathrm{s}$. Figure 8(a) shows an error convergence plot in the L_1 norm for the water height, the curve has slope slightly in access of 0.5, 0.4, 0.47 and 0.47 for modified Rusanov scheme with parameter of control $\alpha^n_{j+\frac{1}{2}}$ being modulated using the Minmod, Superbee, Van Leer and Van Albda limiter, respectively, and 0.56 for the modified Rusanov with constant $\alpha^n_{j+\frac{1}{2}}$. We note that the error in the modified Rusanov scheme with parameter of control $\alpha^n_{j+\frac{1}{2}}$ is less than the error of modified Rusanov scheme with constant parameter. Figure 9(a) shows comparisons on water velocity between the numerical solution with the modified Rusanov scheme, Vazquez's scheme and exact solution using 200 cells and time $t = 1.2$. Figure 9(b) shows the variation of the parameter of control $\alpha^n_{j+\frac{1}{2}}$, this variation has been detected in the area on the computational domain where the rarefaction and shock waves appear.

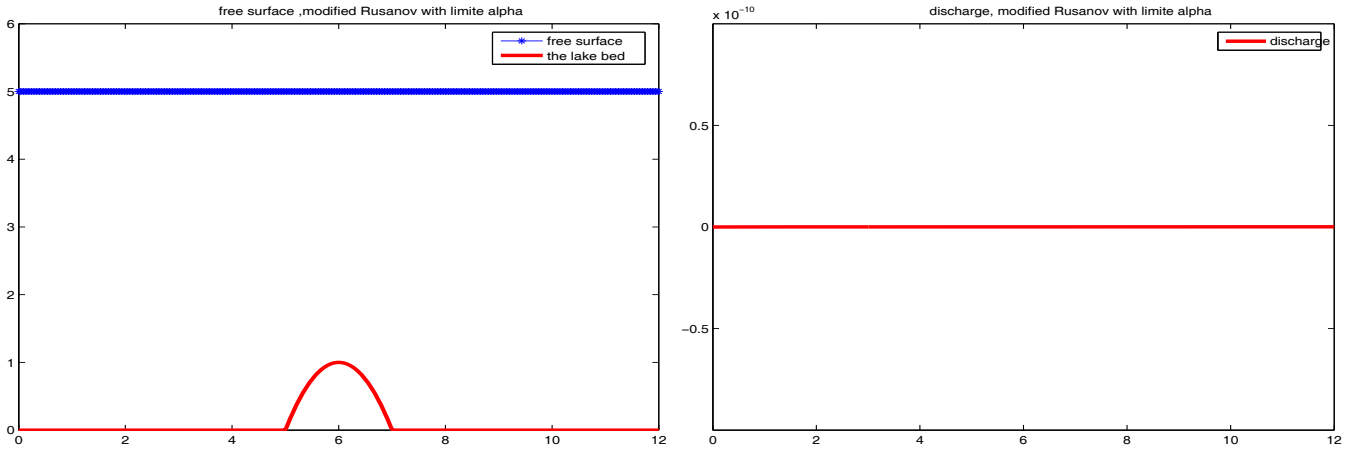

Fig. 10. (a) Free surface. (b) Water discharge for the lake at rest at time $t = 100\,\mathrm{s}$.

4.5 Test 5

This test case is to prove the ability of the modified Rusanov scheme to preserve the correct steady state solutions, the length of the channel is 12 m and the initial conditions are given as follows:

$$\begin{cases} z(x) = \begin{cases} 0 & \text{if} \quad 5 \le x \le 7 \\ 1-(x-6)^2 & \text{otherwise} \end{cases} \\ h_0(x) = 5 - z(x), \\ u_0(x) = 0. \end{cases} \tag{36}$$

We run our scheme using 100 grid points at time $t = 100\,\mathrm{s}$, we note that the modified scheme preserves the C-property, see fig. 10.

5 Numerical results in two dimensions

Similar to one-dimensional tests, we present numerical results for a test problem to check the accuracy and the performance of the proposed finite volume method in two dimensions. As with all explicit time stepping methods the theoretical maximum stable time step Δt is specified according to the CFL condition, see [21]

$$\Delta t \max_i \left(\frac{|\delta C_i|}{A_i} \right) \left[1 + \alpha \frac{M}{m} \right] \frac{M}{2} = Cr, \tag{37}$$

where Cr is a constant to be chosen less than unity and the time step is varied according to eq. (37), with $M = \max_{i,j}(S_{ij}^n)$ and $m = \min_{i,j}(s_{ij}^n)$, where S_{ij}^n is the local Rusanov velocity, A_i is the area of cell C_i, $\alpha = 1.4$ is the parameter of the scheme and $|\delta C_i|$ is the perimeter of the cell C_i.

5.1 Test 1

This test is a subcritical case, it consists of a two-dimensional dam break in a rectangular channel of length 12 m and width 1 m with a gate at $x_0 = 6\,\mathrm{m}$. The initial conditions are given by

	left	right
h	6	2
u	0	0
v	0	0
Z	0	1

.

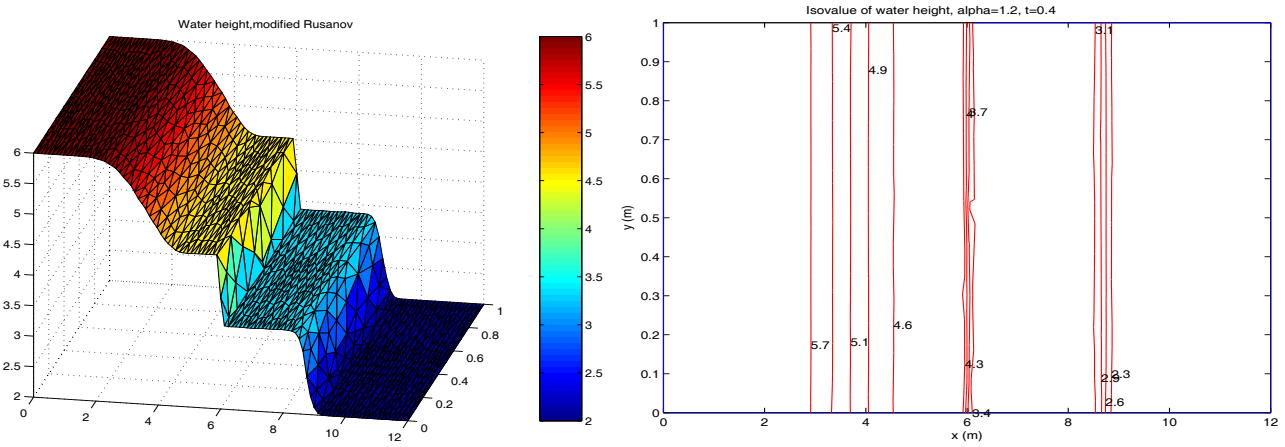

Fig. 11. (a) Water height and (b) its isovalue for dam break over a step computed at $t = 0.4\,\mathrm{s}$ and unstructured mesh 100×10.

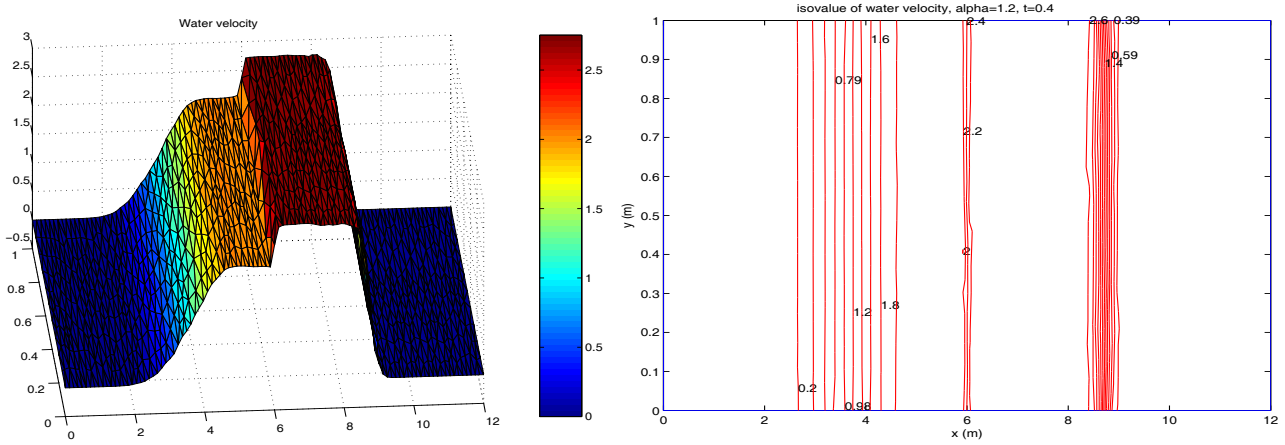

Fig. 12. Water velocity and its isovalue for dam break over a step computed at $t = 0.4\,\mathrm{s}$ and unstructured mesh 100×10.

We simulate this test case with the modified Rusanov scheme at a final time $t = 0.4$ on an unstructured grid 1000 cells. The water height is illustrated in fig. 11(a) and the isovalue of water height is illustrate in fig. 11(b). Figure 12 shows the water velocity and its isovalues. Also, from figs. 11 and 12 we see that the solution is similar to the solution in one dimension and we note that the modified Rusanov scheme captures correctly the discontinuity and the shock wave.

5.2 Test 2

This test is a transcritical case and was presented in [30]. It consists of a two-dimensional dam break in a rectangular channel. The channel is of length 12 m and width 1 m and the initial conditions are given by

	left	right
h	5	1
u	−4	9
v	0	0
Z	0	1

.

We simulate this test case with the modified Rusanov scheme at a final time $t = 0.3\,\mathrm{s}$ on unstructured grids 1000 cells. The water height is illustrated in fig. 13(a) and the isovalues of water height are illustrated in fig. 13(b). Figure 14 shows the water velocity and its isovalues. Also, from figs. 13 and 14 we note that the modified Rusanov scheme captures correctly the discontinuity and the shock wave.

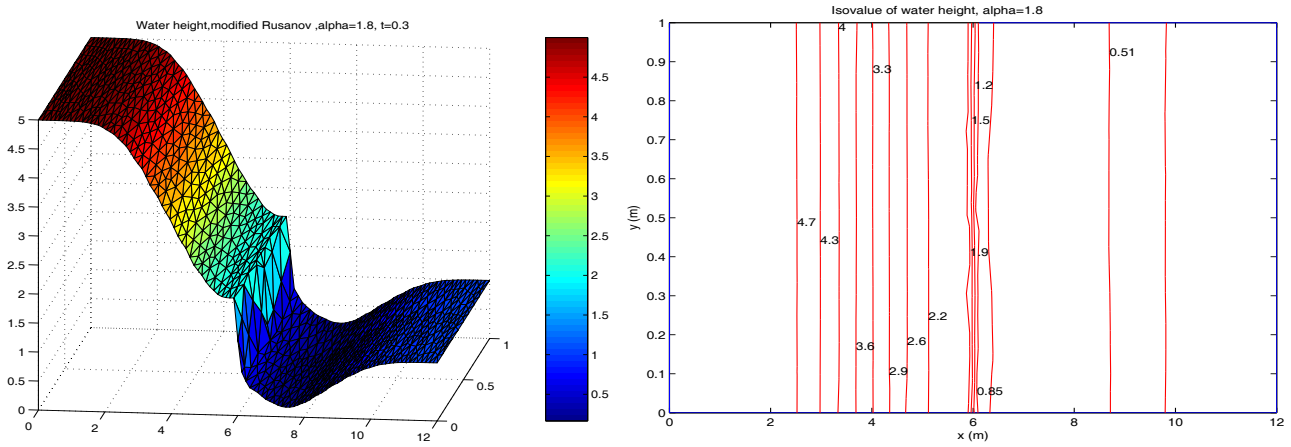

Fig. 13. (a) Water height and (b) its isovalue (right) for dam break over a step computed at $t = 0.3\,\mathrm{s}$ and unstructured mesh 100×10.

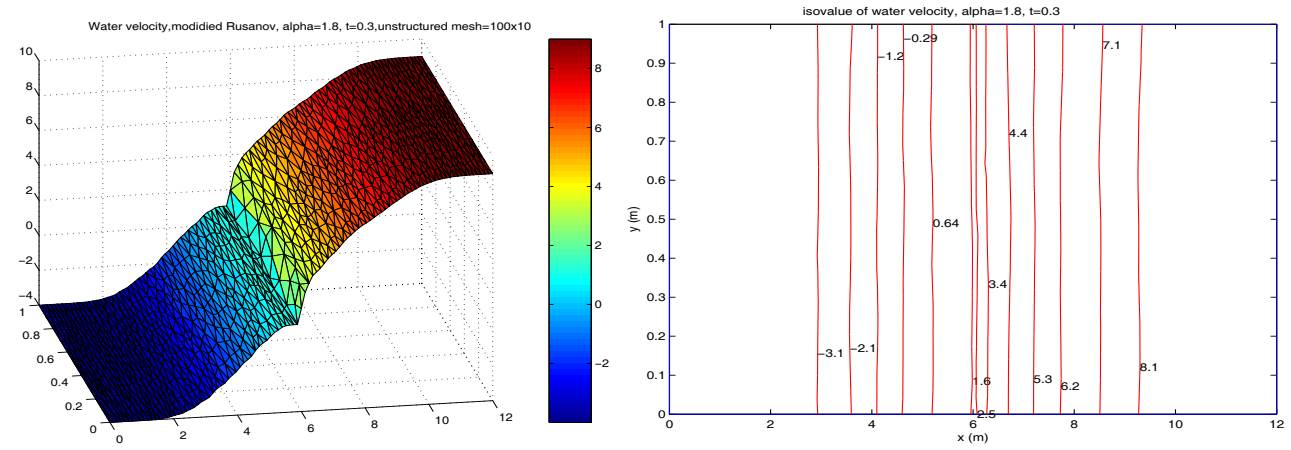

Fig. 14. Water velocity and its isovalue for dam break over a step computed at $t = 0.3\,\mathrm{s}$ and unstructured mesh 100×10.

5.3 Test 3

This supercritical test case consists of a two-dimensional dam break in a rectangular channel. The channel is of length 12 m and width 1 m and the initial conditions are given by

	left	right
h	4	0.1
u	0	0
v	0	0
Z	0	1

.

We simulate this test case with the modified Rusanov scheme at a final time $t = 0.3\,\mathrm{s}$ on unstructured grids 9000 cells. The water height is illustrated in fig. 15(a) and the isovalues of water height is illustrated in fig. 15(b). Figure 16 shows the water velocity and its isovalues. Also, from figs. 15 and 16 we see that the solution is similar to the solution in one dimension, and note that the modified Rusanov scheme captures correctly the rarefaction, discontinuity and the shock wave.

6 The two-phase flow model in one dimension

We consider a one-dimensional single-pressure two-phase flow model which can be written as follows:

$$\frac{\partial \mathbf{W}}{\partial t} + \frac{\partial \mathbf{F}(\mathbf{W})}{\partial x} = \mathbf{Q_1}(\mathbf{W}) + \mathbf{Q_2}(\mathbf{W}), \tag{38}$$

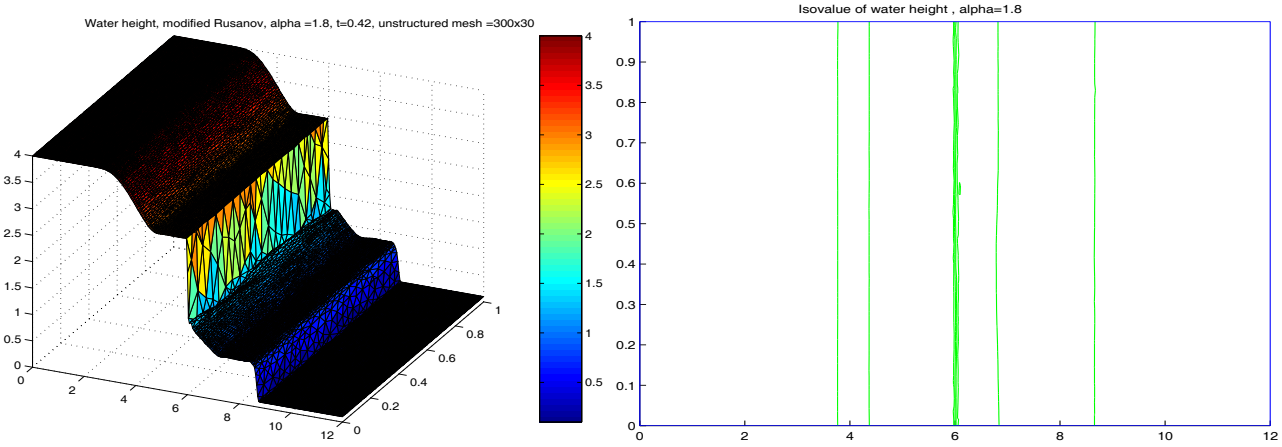

Fig. 15. (a) Water height and (b) its isovalue for dam break over a step computed at $t = 0.3\,\mathrm{s}$ and unstructured mesh 300×30.

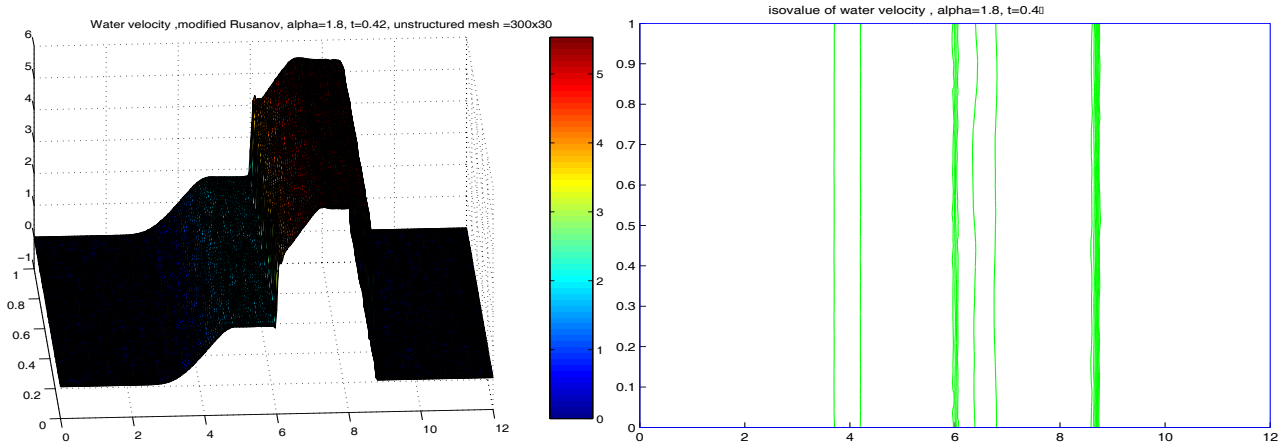

Fig. 16. Water velocity and its isovalue for dam break over a step computed at $t = 0.3\,\mathrm{s}$ and unstructured mesh 300×30.

with $\mathbf{W}$ is conservative variable and $\mathbf{F}(\mathbf{W})$ is flux vector, its given by

$$\mathbf{W}(\mathbf{x},\mathbf{t}) = \begin{pmatrix} \mu_v \rho_v \\ \mu_v \rho_v u_v \\ \mu_l \rho_l \\ \mu_l \rho_l u_l \end{pmatrix}, \qquad \mathbf{F}(\mathbf{W}(\mathbf{x},\mathbf{t})) = \begin{pmatrix} \mu_v \rho_v u_v \\ \mu_v \rho_v u_v^2 \\ \mu_l \rho_l u_l \\ \mu_l \rho_l u_l^2 \end{pmatrix}, \tag{39}$$

where μ is the mass fraction, ρ is the density, u is the velocity, we assume a vapour phase and a liquid phase are subindex by v and l, respectively.

The source term $\mathbf{Q_1}(\mathbf{W})$ is interchange of momentum between both phases and $\mathbf{Q_2}(\mathbf{W})$ represents the effect of the acceleration due the gravity and they are given by

$$\mathbf{Q_1}(\mathbf{W}) = \begin{pmatrix} 0 \\ -\mu_v \dfrac{\partial p}{\partial x} \\ 0 \\ -\mu_l \dfrac{\partial p}{\partial x} \end{pmatrix}, \qquad \mathbf{Q_2}(\mathbf{W}) = \begin{pmatrix} 0 \\ \mu_v \rho_v g \\ 0 \\ \mu_l \rho_l g \end{pmatrix}, \tag{40}$$

where p is the common pressure to both phases, in order to close the system, we apply the closure relation $\mu_v + \mu_l = 1$. The isentropic equation of state for the vapour phase, $p = c\rho_v^{\gamma}$ and an equation of state for the liquid $\rho_l = k_l p^a$, where c, γ, a and k_l are constants. Typical numerical values are: $c = 10^5$, $\gamma = 1.4$, $a = 4.37^{-5}$, and $k_l = 987.57$.

The single pressure two-phase model is non-hyperbolic, the possible solution is lineary unstable and numerical simulation shows the oscillation.

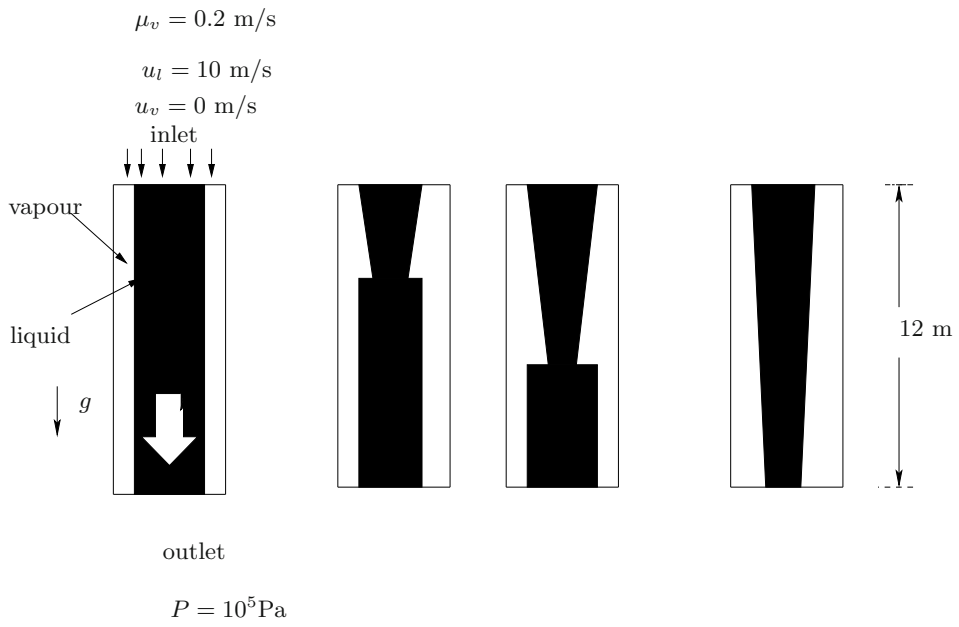

Fig. 17. Sketch of the water faucet.

6.1 A modified Rusanov scheme algorithm

To solve the system (38), we use the splitting strategy presented in [18], in the first step, we treate the gravity source term $\mathbf{Q_2}(\mathbf{W})$ by classical forward Euler time integration as follows:

$$\begin{cases} \dfrac{\partial \tilde{W}}{\partial t} = Q_2(x, \tilde{W}), \\ \tilde{W}(x, t^n) = W^n(x). \end{cases} \tag{41}$$

Then we get $\tilde{W}(x, t^n)$ from $W(x, t^n)$, and we solve the following system by using the modified Rusanov scheme:

$$\begin{cases} \dfrac{\partial W}{\partial t} + \dfrac{\partial F(W)}{\partial x} = Q_1(x, W), \\ W(x, t^n) = \tilde{W}^{n+1}(x). \end{cases} \tag{42}$$

6.2 Application of modified Rusanov scheme to water faucet problem

The water faucet problem [31] consists of a vertical water jet, contained within a cylindrical channel and accelerated under the gravity force. The problem is illustrated schematically in fig. 17. The initial conditions are given by

$\forall x \in [x_0, x_l]$, $\alpha_v(t = 0) = \alpha_0 = 0.2$,
$u_l(t = 0) = 10$, $u_v(t = 0) = 0$,
$p(t = 0) = 10^5$, $\rho_v(t = 0) = 1$,
$\rho_l(t = 0) = 988.0638$,

and the boundary conditions are given by

- ⋆ Inlet($x_0 = 0$): $\mu_v(0, t) = 0.2$, $u_l(0, t) = 10$, $u_v(0, t) = 0$.
- ⋆ Outlet($x_l = 12$): $p(12, t) = 10^5$.

The numerical simulation is computed at time $t = 0.6$ s. Figures 18 and 19 show the vapour volume fraction (void fraction), liquid and vapour velocity. They are computed with different meshes size (from 50 to 200 nodes) for the family of modified Rusanov scheme. We note the void fraction and liquid velocity with our scheme agree with exact solution. Our scheme with 200 nodes is better than the Rusanov's scheme with 3000 nodes. Also, we can see that, when the number of nodes is grater than 200, there are small oscillation at discontinuity of the void fraction. That results from the complex eigenvalues (non-real eigenvalues).

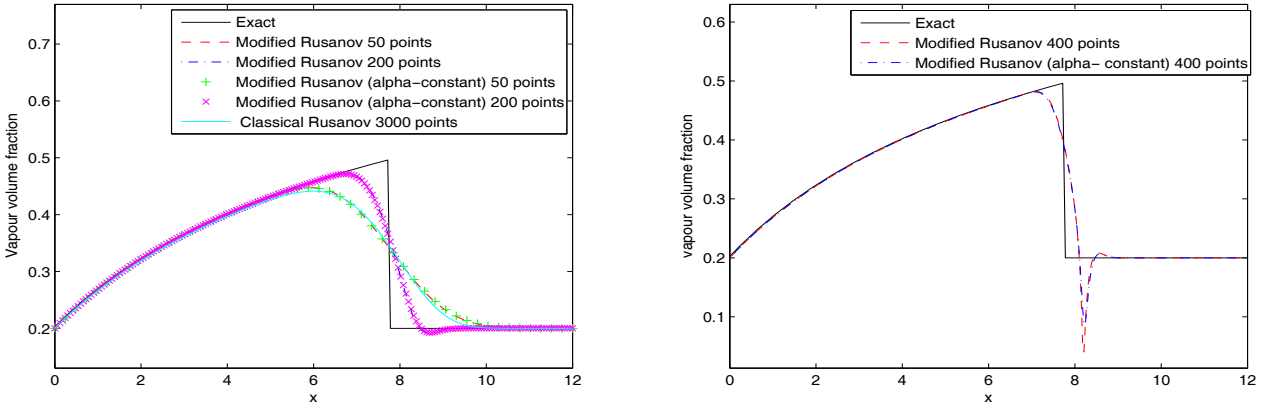

Fig. 18. Vapour fraction at $t = 0.6\,\mathrm{s}$.

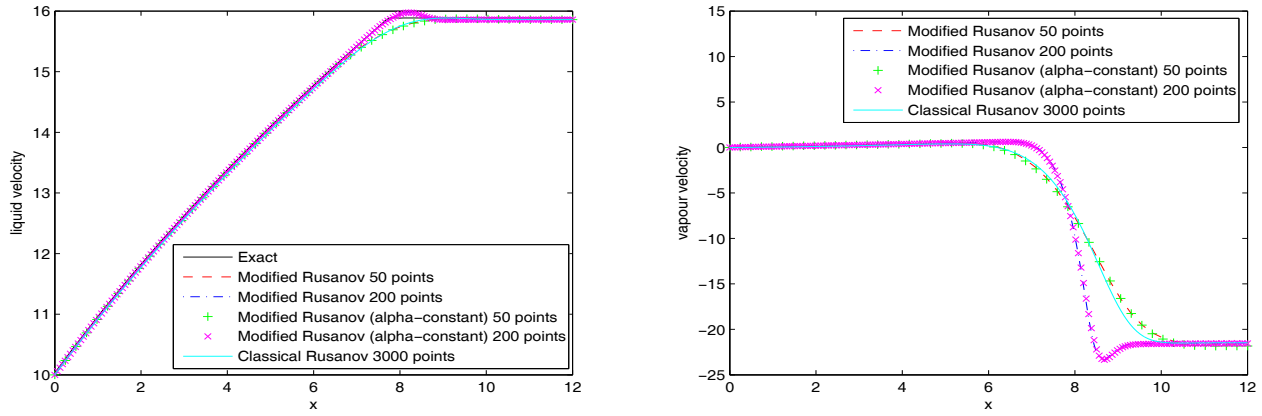

Fig. 19. Liquid velocity and vapour velocity at $t = 0.6\,\mathrm{s}$.

7 Conclusions

In this work paper, we have introduced a modified Rusanov scheme for solving the shallow water equations with source term in one and two dimensions, and one-pressure model of two-phase flows in one space dimension. The proposed method consists of a predictor step and a corrector step. The predictor step depends on a local parameter allowing to control the diffusion. This parameter is modulated using the limiters theory. The corrector step recovers the conservation equations. The comparisons between numerical solution and analytical solution for the one-dimensional dam break over a step and a model problem of two-phase flow have been shown and numerical results have been presented also for two dimensions. This results improve the modified Rusanov scheme and the scheme is very efficient to solve dam break over a step in one and two dimensions, and water faucet problem. The present work can be extended to shallow water equations with bottom friction and Coriolis forces.

References

1. A. Bermudez, M.E. Vazquez, Comput. Fluids **23**, 1049 (1994).
2. P.L. Roe, J. Comput. Phys. **43**, 357 (1981).
3. M.E. Vazquez, J. Comput. Phys. **146**, 497 (1999).
4. J.G. Zhou, D.M. Causon, C.G. Mingham, D.M. Ingram, J. Comput. Phys. **20**, 1 (2001).
5. J. LeVeque Randall, J. Comput. Phys. **146**, 346 (1998).
6. Y. Huang, N. Zhang, Y. Pei, Eng. Appl. Comput. Fluid Mech. **7**, 40 (2013).
7. M.F. Ahmad, M. Mamat, W.B. Wan Nik, A. Kartono, Appl. Math. Comput. Intell. **2**, 95 (2013).
8. F. Zhou, G. Chen, Int. J. Numer. Methods Fluids **73**, 266 (2013).
9. M. Maleewong, Math. Probl. Eng. **2011**, 178491 (2011).
10. D. Aasiorowski, Task Q. **8**, 251 (2012).

11. Szu-Hsien Peng, J. Appl. Math. **2012**, 489269 (2012).
12. S. Tollak Munkejord, Adv. Appl. Math. Mech. **2**, 131 (2010).
13. R.T. Lahey, *The prediction phase of phase distribution and separation phenomena using two-fluid models*, in *Boiling Heat Transfer* (Elsevier Science, 1992) pp. 85–121.
14. S. Tollak Munkejord, Comput. Fluids **36**, 1061 (2007).
15. M.R. Ansari, Nucl. Sci. Technol. **41**, 709 (2004).
16. E. Romenski, D. Drikakis, E. Toro, J. Sci. Comput. **42**, 68 (2010).
17. M. Thanh, A. Izani MDI smail, Phys. Scr. **79**, 065401 (2009).
18. F. Benkhaldoun, *Analysis and validation of a new finite volume scheme for nonhomogeneous systems*, in *Finite Volumes for Complex Applications IV: Problems and Perspectives*, edited by R. Herbin, D. Kroner (2002) pp. 391–402.
19. F. Benkhaldoun, K. Mohamed, L. Quivy, *A finite volume two steps flux scheme for 1D and 2D non homogeneous systems*, in *FVCA4* (Hermes Science Publishing, 2005) pp. 423–433.
20. K. Mohamed, M. Seaid, M. Zahri, J. Comput. Appl. Math. **237**, 614 (2013).
21. K. Mohamed, *Simulation numérique en volume finis, de problémes d'écoulements multidimensionnels raides, par un schéma de flux á deux pas*, Dissertation, University of Paris 13 (2005).
22. F. Benkhaldoun, K. Mohamed, M. Seaid, *A generalized Rusanov method for Saint-Venant equations with variable horizontal density, FVCA*, in *International Symposium, Prague, June 6-10* (2011) pp. 96–112.
23. K. Mohamed, H. Shaban, Int. J. Appl. Math. Stat. **31**, 96 (2013).
24. K. Mohamed, J. Comput. Fluids **104**, 9 (2014).
25. J. LeVeque Randall, *Numerical Methods for Conservation Laws*, in *Lectures in Mathematics* (ETH Zürich, 1992).
26. P.K. Sweby, SIAM J. Numer. Anal. **21**, 995 (1984).
27. A. Bermudez, A. Dervieux, J.-A. Desideri, M.E. Vazquez, Comput. Methods Appl. Mech. Eng. **155**, 49 (1998).
28. V.V. Rusanov, J. Comput. Math. Phys. USSR **1**, 267 (1961).
29. F. Alcrudo, F. Benkhaldoun, Comput. Fluids **30**, 643 (2001).
30. F. Benkhaldoun, I. Elmahi, M. Seaid, J. Comput. Phys. **226**, 180 (2007).
31. V.H. Ransom, *Numerical benchmark tests*, in *Multiphase Science and Technology*, edited by G.F. Hewitt, J.M. Delhay, N. Zuber (Hemisphere, Washington, 1987).